

To Use or Not to Use a Universal Force Field

Denan Li,^{†,¶} Jiyuan Yang,^{†,¶} Xiangkai Chen,^{†,‡} Lintao Yu,[†] and Shi Liu^{*,†,‡}

[†]*Department of Physics, School of Science, Westlake University, Hangzhou, Zhejiang
310030, China*

[‡]*Institute of Natural Sciences, Westlake Institute for Advanced Study, Hangzhou, Zhejiang
310024, China*

[¶]*These authors contributed equally*

E-mail: liushi@westlake.edu.cn

Abstract

Artificial intelligence (AI) is revolutionizing scientific research, particularly in computational materials science, by enabling more accurate and efficient simulations. Machine learning force fields (MLFFs) have emerged as powerful tools for molecular dynamics (MD) simulations, potentially offering quantum-mechanical accuracy with the efficiency of classical MD. This Perspective evaluates the viability of universal MLFFs for simulating complex materials systems from the standpoint of a potential practitioner. Using the temperature-driven ferroelectric-paraelectric phase transition of PbTiO_3 as a benchmark, we assess leading universal force fields, including CHGNet, MACE, M3GNet, and GPTFF, alongside specialized models like UniPero. While universal MLFFs trained on PBE-derived datasets perform well in predicting equilibrium properties, they largely fail to capture realistic finite-temperature phase transitions under constant-pressure MD, often exhibiting unphysical instabilities. These shortcomings stem from inherited biases in exchange-correlation functionals and limited generalization to anharmonic interactions governing dynamic behavior. However, fine-tuning universal models or employing system-specific MLFFs like UniPero successfully restores predictive accuracy. We advocate for hybrid approaches combining universal pretraining with targeted optimization, improved error quantification frameworks, and community-driven benchmarks to advance MLFFs as robust tools for computational materials discovery.

Artificial intelligence (AI) is rapidly emerging as the fifth paradigm of scientific research, joining the established paradigms of experiments, theory, computation, and data. This transformative technology is fundamentally reshaping the nature of scientific inquiry and has the potential to significantly accelerate the pace of scientific discovery. The recognition of AI’s contributions to science, highlighted by its acknowledgment in the 2024 Nobel Prizes in both Physics and Chemistry,^{1,2} firmly establishes the era of “AI for Science.” In materials science, AI holds immense potential to elucidate complex structure-property relationships, thereby enhancing and expediting the processes of materials discovery and design.

In this Perspective, we primarily focus on machine learning force fields (MLFFs) for classical molecular dynamics (MD) simulations. Classical MD simulations employ parameterized interatomic potentials, enabling computationally efficient exploration of dynamic processes across large temporal and spatial scales. These simulations not only reveal atomic-level mechanisms but also provide foundational data for coarse-grained models,^{3,4} further extending their importance in multiscale simulations. Classical MD simulations have long been an indispensable tool for computer-aided drug design (CADD), driven by classical force fields like CHARMM, AMBER, and GROMOS, which accurately describe biomolecular interactions in proteins and nucleic acids.^{5,6} In contrast, the adoption of MD in computer-aided materials discovery (CAMD) lags behind due to the absence of universal force fields capable of handling diverse elements, especially transition-metal oxides and complex alloys. This challenge mainly stems from the high-dimensional potential energy surface (PES) inherent in multielement systems, where traditional analytical functionals struggle to balance accuracy and generality.

The emergence of MLFFs is transforming the field of MD simulations. By leveraging advanced techniques such as deep neural networks (DNNs) and graph neural networks (GNNs), MLFFs achieve quantum-mechanical accuracy while retaining the computational efficiency of classical MD. The standard protocol for developing an MLFF involves training the model on databases computed using density functional theory (DFT), which include energies, atomic

forces, and virial tensors across a diverse set of atomic configurations. Inspired by the success of large language models represented by OpenAI’s ChatGPT, recent efforts have introduced several “atomistic foundational models”,^{7–15} designed to serve as universal force fields for enabling MD simulations across a wide range of material systems. Notable examples include M3GNet,⁷ CHGNet,⁸ and MACE,⁹ which are based on GNN architectures and are trained on extensive, materials science databases.^{16–18} Proprietary advancements include GNoME,¹⁹ built upon E(3)-equivariant graph neural networks, and PFP,²⁰ which leverages the TeaNet architecture²¹ to combine attention mechanisms with graph-based atomic representations. The GPTFF model¹⁰ integrates GNN and transformer architectures with attention mechanisms, is trained on the proprietary Atomly database. The DPA-2 model¹² positions itself as a pre-trained model covering more than 90 elements. It is designed to significantly reduce downstream data requirements by leveraging transfer learning, enabling efficient on-demand fine-tuning to create tailored models for specific materials of user interest. These developments mark a paradigm shift toward general-purpose MLFFs capable of simulating complex multielement systems, from battery electrolytes to high-entropy alloys. Recently, Riebesell *et al.* developed **Matbench Discovery**, an evaluation framework for ML models, applied as pre-filters for high-throughput searches of stable inorganic crystals.²²

Here, we take the perspective of potential practitioners and pose an important question: how do I select the most suitable atomistic foundational model, or universal force field, to study the materials system of my interest? Naturally, the choice is highly case-dependent, as the tasks of different researchers vary widely. However, a common requirement often involves running MD simulations spanning tens or hundreds of picoseconds to investigate the dynamics of materials of interest. After all, the distinctive advantage of MD simulations over static computational approaches lies in their ability to reveal time-dependent atomic behaviors and emergent properties that would otherwise remain inaccessible. While existing benchmarks primarily emphasize energy and force prediction accuracy, this Perspective argues that the true measure of an MLFF’s utility lies in its performance under realistic MD

conditions. Specifically, the focus should be on how well the model performs during finite-temperature simulations over tens to hundreds of picoseconds, where accurately capturing dynamical properties, such as phase transition kinetics, is critical. Therefore, selecting a model should not only depend on its static accuracy but also on its ability to reliably reproduce the dynamic behavior of materials under practical conditions.

In the following (admittedly not comprehensive) performance assessment, we use the temperature-driven ferroelectric-paraelectric phase transition of PbTiO_3 as a test case, referred to as the **PT0-test**. As a prototypical ferroelectric material, PbTiO_3 is one of the most extensively studied perovskite oxides. Its ground state adopts a tetragonal phase (space group $P4mm$) characterized by spontaneous electrical polarization, which transitions to a nonpolar cubic phase (space group $Pm\bar{3}m$) at temperatures above 760 K, as observed in experiments.²³ The tetragonal phase features a short axis, a , and a long axis, c , with the tetragonality defined by the ratio c/a , which correlates with the magnitude of the polarization. The energy difference between the ferroelectric and paraelectric phases, determined by DFT calculations at zero Kelvin, is 16 meV/atom. This moderate energy difference falls within the accuracy range of typical MLFFs. Furthermore, the sub-800K transition temperature allows for direct MD validation without requiring extrapolation to extreme thermal regimes (>1000 K), where anharmonic effects could introduce significant complexities. For these reasons, we consider the **PT0-test** an ideal benchmark: it is sufficiently complex to reveal potential limitations of MLFFs in modeling phase transition, yet tractable enough to enable systematic error analysis.

The MLFFs selected for this benchmark include CHGNet, GPTFF, MACE, M3GNet, ORB, and SevenNet. Unfortunately, our request for access to EquiformerV2-OMat^{18,24} was denied. Table 1 provides an overview of these MLFFs, detailing the model versions used in our tests, their training datasets, the number of trainable parameters, and the mean absolute error (MAE) for energy and forces during training. Additionally, we evaluate UniPero, a “professional model” designed as a universal force field for perovskite oxides, covering 14

metal elements.²⁵ It mainly follows the architecture of DPA-1,²⁶ an earlier version of DPA-2.

We begin by determining the ground-state structure of the tetragonal phase of PTO through structural optimizations employing various MLFFs. Figure 1 compares the lattice parameter a and the tetragonality (c/a) predicted by these MLFFs with results from standard exchange-correlation (XC) functionals, including LDA, PBE, and PBEsol. The values are also summarized in Table 2. It is well known that the PBE functional significantly overestimates the c/a ratio (experimental value: 1.06), yielding a value of 1.23, whereas PBEsol gives a closer estimate of 1.10. This discrepancy explains why universal MLFFs trained on PBE-based databases, such as CHGNet, M3GNet, and MACE, inherit this bias, predicting c/a ratios even larger than that from PBE itself. The exception is UniPero, which aligns with PBEsol due to its training on PBEsol-derived data. This reveals an expected limitation in universal force fields: their accuracy is inherently tied to the XC functional used in their training database. For systems like PTO, where even conventional XC functionals struggle to reproduce key properties like tetragonality, selecting an appropriate functional *a priori* becomes essential for developing reliable MLFFs. To address this limitation, we demonstrate that fine-tuning an existing MLFF with a more suitable database can recover accuracy. For instance, retraining the MACE model on the PBEsol-based dataset used for UniPero yields a fine-tuned force field, denoted as MACE-FT. As shown in Figure 1, MACE-FT predicts a ground-state structure in excellent agreement with PBEsol.

We calculate the phonon spectrum of the optimized tetragonal PTO for each MLFF using the finite-displacement method implemented in Phonopy package,²⁷ with atomic forces evaluated directly by the respective MLFF. Despite their overestimated tetragonality, most MLFFs including CHGNet, MACE, and SevenNet generate phonon spectra free of imaginary frequencies (Fig. 2), confirming dynamical stability. As shown in Fig. 2, the phonon spectra of CHGNet, GPTFF, MACE, and SevenNet closely align with the PBE reference. In contrast, the phonon spectrum of M3GNet exhibits instability across the Brillouin zone; ORB displays localized instabilities near the Γ point, characterized by weak imaginary frequencies (below

20 cm^{-1}), and also predicts notably flat bands for low-frequency phonons. Both UniPero and MACE-FT accurately reproduce the PBEsol phonon spectrum. Since phonon spectra are highly sensitive to the second derivatives of the PES near equilibrium, this benchmark highlights that most MLFFs effectively capture the local curvature of the PES corresponding to their parent XC functional.

One might expect that an accurate representation of the local energy landscape near the ground-state geometry would ensure that most MLFFs are at least qualitatively reliable for finite-temperature lattice dynamics simulations. However, as shown in Fig. 3, nearly all universal force fields fail the `PT0-test`, proving unable to reproduce the temperature-driven tetragonal-to-cubic phase transition in constant-pressure constant-temperature (*NPT*) MD simulations. For instance, MD simulations using CHGNet, M3GNet, MACE, and SevenNet exhibit abrupt instabilities above a critical temperature, causing the system to collapse into a disordered, molten state devoid of a crystalline lattice. Before reaching this molten phase, CHGNET, MACE, and SevenNet stabilize a persistent supertetragonal phase. Although the ORB reproduces the tetragonal-to-cubic phase transition at ≈ 1100 K, it erroneously predicts a non-existent cubic-to-tetragonal transition at a higher temperature. Among the universal force fields tested, GPTFF appears to be the only one that predicts a temperature-driven (super)tetragonal-to-cubic phase transition. These results reveal another limitation: accurately capturing the local curvature near the ground state does not necessarily translate to correctly modeling anharmonic interactions and the free-energy landscapes that govern temperature-dependent structural transitions in complex oxides. In contrast, both UniPero and MACE-FT successfully reproduce the expected ferroelectric-paraelectric phase transition, though the Curie temperature is underestimated by approximately 160 K compared to the experimental value.

Running *NPT* simulations imposes stringent accuracy requirements on MLFFs, demanding precise parameterization to capture pressure-density relationships and accurate computation of virial contributions essential for pressure control. However, if an MLFF is primarily

trained on equilibrium configurations (ground-state structures), it may lack the generalizability to handle the dynamic volume fluctuations inherent to NPT ensembles. To mitigate this challenge, we conduct a controlled validation test using constant-volume, constant-temperature (NVT) MD simulations, fixing the lattice constants of PTO to experimental values. This approach eliminates volume relaxation, simplifying the system while still allowing us to probe temperature-driven phase transitions. Notably, most MLFFs including CHGNet, MACE, MACE-FT, ORB, SevenNet, and UniPero successfully predict the ferroelectric-to-paraelectric transition, with the spontaneous polarization along the long axis (P_z) dropping to near zero at ≈ 1100 K (Fig. 4). In contrast, M3GNet and GPTFF exhibit significant deviations, predicting Curie temperatures far below expectations. These results indicate that under constrained NVT conditions, most MLFFs capture finite-temperature lattice behavior, as the reduced degrees of freedom simplify the energy landscape.

Finally, we briefly discuss the computational efficiency of the tested models, as shown in Fig. 5. It is noted that only SevenNet and the DPA-based UniPero are designed for multi-GPU parallelism, a crucial feature for large-scale MD simulations. Since some models do not support multi-GPU parallelism or specialized MD packages like LAMMPS,²⁸ the speed test is conducted on a single GPU using the Atomic Simulation Environment (ASE),²⁹ which integrates each MLFF as a calculator. Therefore, the reported speed data are for reference only, as the optimal performance of a model could be improved with careful tuning. Our benchmark reveals that most models have yet to fully optimize their performance for GPU acceleration. For instance, M3GNet’s slower computational performance arises from unresolved GPU compatibility issues in our cluster which defaults to CPU execution rather than leveraging GPU acceleration. While this issue might be resolved with proper settings, it highlights a potential engineering burden for users adopting universal force fields at this stage. Notably, ORB outperforms UniPero despite having a larger parameter count, leveraging the TensorFloat32 (TF32) data format for enhanced efficiency. UniPero, originally based on the DPA-1 architecture with the self-attention mechanism, demonstrated significantly

improved speed when simplified to a smooth edition of deep potential (DeepPot-SE)³⁰ and further compressed using techniques including tabulated inference, operator merging, and precise neighbor indexing, making it the fastest model in our benchmarks. Furthermore, by integrating this optimized model into LAMMPS and fully harnessing multi-GPU parallelism, we successfully conducted an MD simulation of 240,000 atoms across 48 GPUs, achieving an impressive computational speed of approximately 42 steps per second.

There is no doubt that we are entering an era where AI is transforming scientific inquiry, particularly in computational materials science. While this Perspective does not attempt to chart the entire frontier, it addresses a fundamental question posed in its title: Should we use a universal force field? Our benchmarks suggest a qualified “yes,” provided their limitations are carefully considered. Many universal MLFFs demonstrate remarkable accuracy in predicting phonon spectra and equilibrium properties. However, their reliability declines in large-scale, finite-temperature MD simulations, where computational cost and stability pose significant challenges. A deeper issue lies not in the ML frameworks themselves but in their training data, most rely on semilocal density functionals like PBE, which are known to fail in many material systems. This dependence risks propagating systematic errors into MLFFs, particularly when used for high-throughput screening or structural searches. Our benchmark results underscore the need for improved data sources and hybrid approaches that integrate universal pretraining with system-specific fine-tuning. Advancing MLFFs requires incorporating beyond-PBE methods, enhancing computational efficiency, and developing robust error quantification frameworks. To ensure MLFFs perform reliably in complex, real-world applications, open benchmarks and community-driven validation are essential. Rather than critiquing any specific model, the goal is to refine universal MLFFs into versatile, trustworthy tools that complement specialized approaches, unlocking AI’s full potential in computational materials discovery.

Methods

All calculations are performed using the Atomic Simulation Environment (ASE),²⁹ with each MLFF integrated as an ASE calculator to compute energy, forces, and stress. To simulate the temperature-driven phase transition of PbTiO_3 , a $5 \times 5 \times 5$ supercell containing 625 atoms is constructed from the ground-state structure. MD simulations are carried out in the isothermal-isobaric (NPT) ensemble using a Parrinello–Rahman barostat coupled with a Nosé–Hoover thermostat. At each temperature, the simulation runs with a 2 fs timestep for 50,000 steps, totaling 100 ps. The last 50 ps of the trajectory is used to compute the averaged lattice constants. For the NVT ensemble simulation, the same $5 \times 5 \times 5$ supercell is used, with lattice parameters fixed at their experimental values measured at room temperature. Langevin dynamics are employed with a 2 fs timestep for 50,000 steps. For performance benchmarking, all computations are performed on a single V100-SXM2-16G GPU, with each data point averaged over three independent runs.

Acknowledgments

We acknowledge the supports from National Natural Science Foundation of China (92370104) and Westlake Education Foundation. The computational resource is provided by Westlake HPC Center.

References

- (1) The Royal Swedish Academy of Sciences The Nobel Prize in Physics 2024. 2024; <https://www.nobelprize.org/prizes/physics/2024/summary/>, [Accessed: 2025-03-10].
- (2) The Royal Swedish Academy of Sciences The Nobel Prize in Chemistry 2024. 2024; <https://www.nobelprize.org/prizes/chemistry/2024/summary/>, [Accessed: 2025-03-10].

- (3) Schilling, T. Coarse-grained modelling out of equilibrium. *Phys. Rep.* **2022**, *972*, 1–45.
- (4) Sun, T.; Minhas, V.; Korolev, N.; Mirzoev, A.; Lyubartsev, A. P.; Nordenskiöld, L. Bottom-up coarse-grained modeling of DNA. *Front. Mol. Biosci.* **2021**, *8*, 645527.
- (5) Liebl, K.; Zacharias, M. The development of nucleic acids force fields: From an unchallenged past to a competitive future. *Biophys. J.* **2023**, *122*, 2841–2851.
- (6) Samuel Russell, P. P.; Alaeen, S.; Pogorelov, T. V. In-cell dynamics: The next focus of all-atom simulations. *J. Phys. Chem. B* **2023**, *127*, 9863–9872.
- (7) Chen, C.; Ong, S. P. A universal graph deep learning interatomic potential for the periodic table. *Nat. Comput. Sci.* **2022**, *2*, 718–728.
- (8) Deng, B.; Zhong, P.; Jun, K.; Riebesell, J.; Han, K.; Bartel, C. J.; Ceder, G. CHGNet as a pretrained universal neural network potential for charge-informed atomistic modelling. *Nat. Mach. Intell.* **2023**, *5*, 1031–1041.
- (9) Batatia, I. et al. A foundation model for atomistic materials chemistry. *Preprint at arXiv* **2023**, arXiv:2401.00096.
- (10) Xie, F.; Lu, T.; Meng, S.; Liu, M. GPTFF: A high-accuracy out-of-the-box universal AI force field for arbitrary inorganic materials. *Sci. Bull.* **2024**, *69*, 3525–3532.
- (11) Neumann, M.; Gin, J.; Rhodes, B.; Bennett, S.; Li, Z.; Choubisa, H.; Hussey, A.; Godwin, J. Orb: A fast, scalable neural network potential. *Preprint at arXiv* **2024**, arXiv:2410.22570.
- (12) Zhang, D. et al. DPA-2: a large atomic model as a multi-task learner. *npj Comput. Mater.* **2024**, *10*, 293.
- (13) Kim, J.; Kim, J.; Kim, J.; Lee, J.; Park, Y.; Kang, Y.; Han, S. Data-efficient multifidelity training for high-fidelity machine learning interatomic potentials. *J. Am. Chem. Soc.* **2024**, *147*, 1042–1054.

- (14) Yin, B.; Wang, J.; Du, W.; Wang, P.; Ying, P.; Jia, H.; Zhang, Z.; Du, Y.; Gomes, C. P.; Duan, C.; Xiao, H.; Henkelman, G. AlphaNet: Scaling Up Local Frame-based Atomistic Foundation Model. *Preprint at arXiv* **2025**, arXiv:2501.07155.
- (15) Yang, H. et al. Mattersim: A deep learning atomistic model across elements, temperatures and pressures. *Preprint at arXiv* **2024**, arXiv:2405.04967.
- (16) Jain, A.; Ong, S. P.; Hautier, G.; Chen, W.; Richards, W. D.; Dacek, S.; Cholia, S.; Gunter, D.; Skinner, D.; Ceder, G.; Persson, K. A. Commentary: The Materials Project: A materials genome approach to accelerating materials innovation. *APL Mater.* **2013**, *1*, 011002.
- (17) Schmidt, J.; Wang, H.-C.; Cerqueira, T. F.; Botti, S.; Marques, M. A. A dataset of 175k stable and metastable materials calculated with the PBEsol and SCAN functionals. *Sci. Data* **2022**, *9*, 64.
- (18) Barroso-Luque, L.; Shuaibi, M.; Fu, X.; Wood, B. M.; Dzamba, M.; Gao, M.; Rizvi, A.; Zitnick, C. L.; Ulissi, Z. W. Open materials 2024 (omat24) inorganic materials dataset and models. *Preprint at arXiv* **2024**, arXiv:2410.12771.
- (19) Merchant, A.; Batzner, S.; Schoenholz, S. S.; Aykol, M.; Cheon, G.; Cubuk, E. D. Scaling deep learning for materials discovery. *Nature* **2023**, *624*, 80–85.
- (20) Takamoto, S. et al. Towards universal neural network potential for material discovery applicable to arbitrary combination of 45 elements. *Nat. Commun.* **2022**, *13*, 2991.
- (21) Takamoto, S.; Izumi, S.; Li, J. TeaNet: Universal neural network interatomic potential inspired by iterative electronic relaxations. *Comput. Mater. Sci.* **2022**, *207*, 111280.
- (22) Riebesell, J.; Goodall, R. E.; Benner, P.; Chiang, Y.; Deng, B.; Lee, A. A.; Jain, A.; Persson, K. A. Matbench Discovery—A framework to evaluate machine learning crystal stability predictions. *Preprint at arXiv* **2023**, arXiv:2308.14920.

- (23) Shirane, G.; Hoshino, S. On the phase transition in lead titanate. *J. Phys. Soc. Jpn.* **1951**, *6*, 265–270.
- (24) Liao, Y.-L.; Wood, B.; Das, A.; Smidt, T. EquiformerV2: Improved equivariant transformer for scaling to higher-degree representations. *Preprint at arXiv* **2023**, arXiv:2306.12059.
- (25) Wu, J.; Yang, J.; Liu, Y.-J.; Zhang, D.; Yang, Y.; Zhang, Y.; Zhang, L.; Liu, S. Universal interatomic potential for perovskite oxides. *Phys. Rev. B* **2023**, *108*, L180104.
- (26) Zhang, D.; Bi, H.; Dai, F.-Z.; Jiang, W.; Liu, X.; Zhang, L.; Wang, H. Pretraining of attention-based deep learning potential model for molecular simulation. *npj Comput. Mater.* **2024**, *10*, 94.
- (27) Togo, A.; Chaput, L.; Tadano, T.; Tanaka, I. Implementation strategies in phonopy and phono3py. *J. Phys. Condens. Matter* **2023**, *35*, 353001.
- (28) Plimpton, S. Fast Parallel Algorithms for Short-Range Molecular Dynamics. *J. Comput. Phys.* **1995**, *117*, 1–19.
- (29) Hjorth Larsen, A. et al. The atomic simulation environment—a Python library for working with atoms. *J. Phys.:Condens. Matter* **2017**, *29*, 273002.
- (30) Zhang, L.; Han, J.; Wang, H.; Saidi, W. A.; Car, R.; Weinan, E. End-to-End Symmetry Preserving Inter-Atomic Potential Energy Model for Finite and Extended Systems. Proceedings of the 32nd International Conference on Neural Information Processing Systems. Red Hook, NY, USA, 2018; pp 4441–4451.
- (31) Park, Y.; Kim, J.; Hwang, S.; Han, S. Scalable parallel algorithm for graph neural network interatomic potentials in molecular dynamics simulations. *J. Chem. Theory Comput.* **2024**, *20*, 4857–4868.

- (32) Meyer, B.; Vanderbilt, D. *Ab Initio* Study of Ferroelectric Domain Walls in PbTiO_3 .
Phys. Rev. B **2002**, *65*, 104111.
- (33) Mabud, S.; Glazer, A. Lattice parameters and birefringence in PbTiO_3 single crystals.
J. Appl. Crystallogr. **1979**, *12*, 49–53.

Table 1: Summary of key properties of various MLFFs used for PT0-test.

Model	Version	Training Set (Size)	Parameters	Energy MAE (meV/atom)	Force MAE (meV/Å)
CHGNet ⁸	0.3.0	MPtrj (146K)	413K	26	60
GPTFF ¹⁰	v2	Atomly (37.8M)	502K	32	71
M3GNet ⁷	MP-2021.2.8-PES	MPF-2021.2.8 (62.8K)	228K	18.7	63
MACE ⁹	MP-0b-medium	MPtrj (146K)	4.69M	20	45
ORB ¹¹	orb-v2	MPtrj (146K) + Alexandria (3.1M)	25.2M	/	/
SevenNet ³¹	7net-l3i5	MPtrj (146K)	1.17M	8.3	29
UniPero ²⁵	v1	Customized (19K)	≈500K	1.75	54

Notes: Some models have been updated since their initial publication. When available, the latest version is used, and the energy and force mean absolute errors (MAEs, if reported) are taken from the latest version if available; otherwise, they are taken from the original references. Abbreviations: MPtrj = Materials Project trajectories; MPF = Materials Project structure relaxations

Table 2: Lattice parameters (a and c), tetragonality (c/a) of the tetragonal PbTiO_3 phase, and the energy difference (ΔE) between the tetragonal and cubic phases predicted by different MLFFs. Experimental and DFT results are also included for comparison.

Model	a (Å)	c (Å)	c/a	ΔE (eV/f.u.)
CHGNet	3.80	5.01	1.32	0.24
GPTFF	3.79	4.88	1.29	0.25
M3GNet	3.80	4.92	1.30	0.16
MACE	3.84	4.83	1.26	0.19
ORB	3.83	4.87	1.27	0.21
SevenNet	3.84	4.79	1.25	0.21
MACE-FT	3.89	4.16	1.07	0.08
UniPero	3.88	4.21	1.08	0.09
LDA ³²	3.86	4.04	1.05	
PBE	3.85	4.73	1.23	0.20
PBEsol	3.87	4.20	1.08	0.08
Exp. ³³	3.90	4.15	1.06	

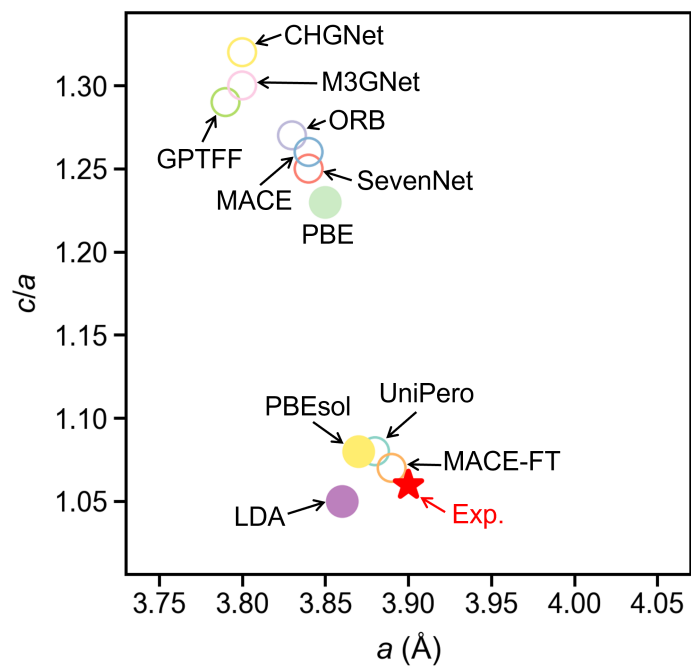


Figure 1: Lattice parameter a and tetragonality (c/a) of ground-state PbTiO_3 predicted by various MLFFs and exchange-correlation functionals.

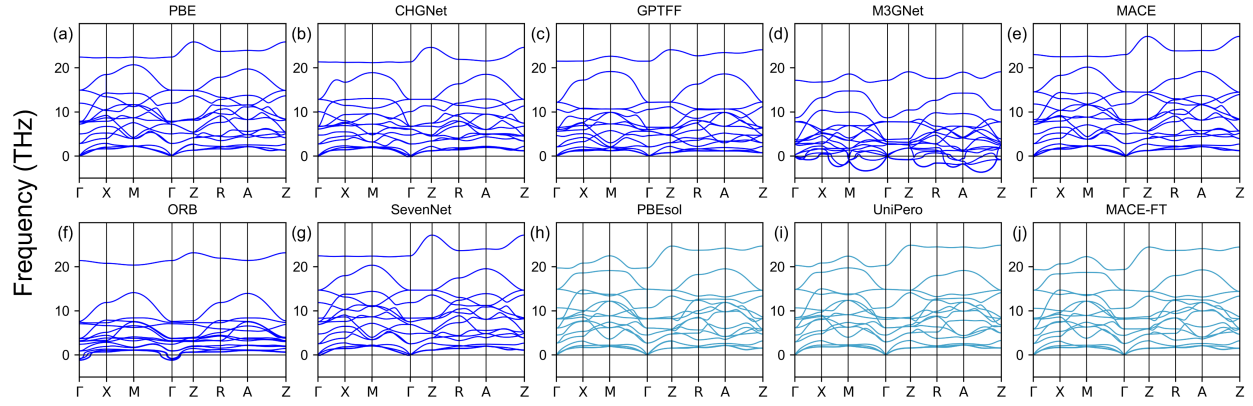


Figure 2: Phonon spectra of PbTiO_3 calculated using various MLFFs, each based on the optimized ground-state tetragonal structure. The spectra obtained from PBE and PBEsol are also included for comparison. UniPero and MACE-FT are trained on a PBEsol-derived database.

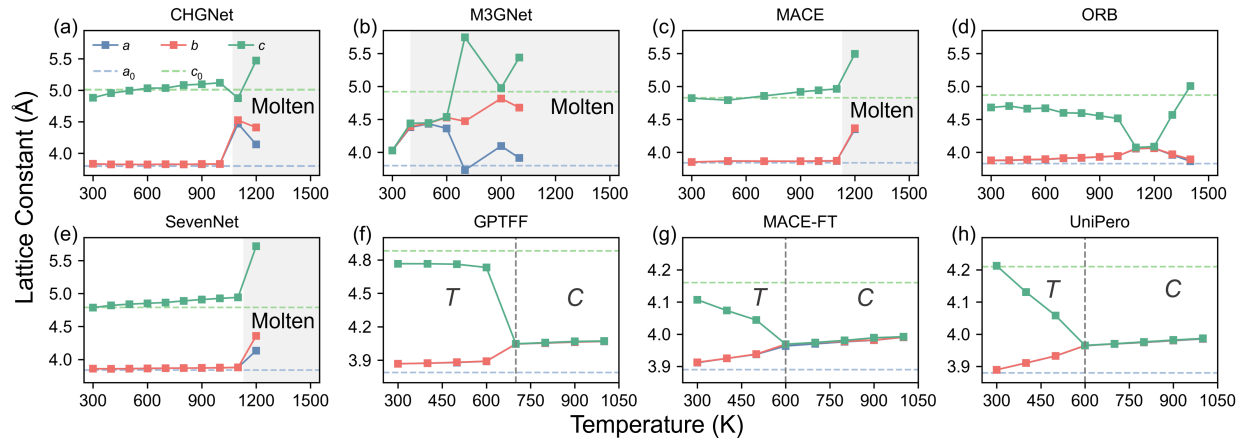


Figure 3: Temperature-dependent lattice constants (a and c) obtained from NPT MD simulations using various MLFFs. The dashed lines indicate the ground-state lattice parameters (a_0 and c_0) of tetragonal PbTiO_3 for each MLFF.

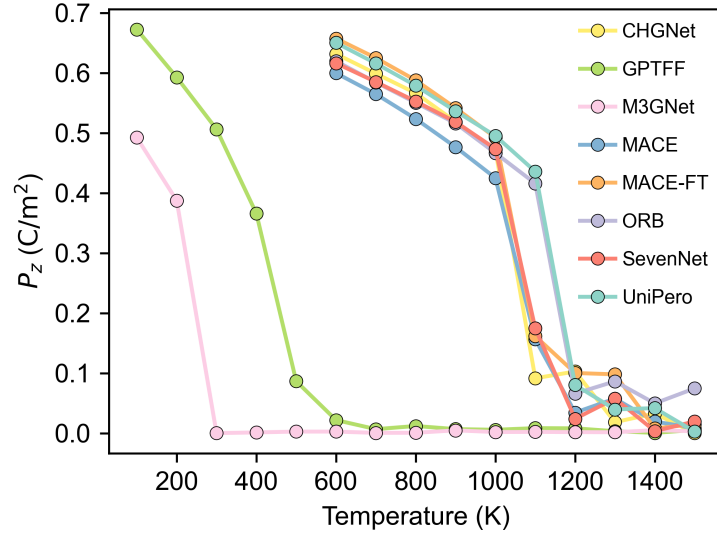


Figure 4: Temperature-dependent spontaneous polarization along the c -axis (P_z) obtained from NVT MD simulations, with lattice parameters fixed to the experimental room-temperature values ($a = 3.90 \text{ \AA}$, $c = 4.15 \text{ \AA}$). At high temperatures, the polarization does not fully converge to zero due to the imposed tetragonality constraint ($c/a = 1.06$).

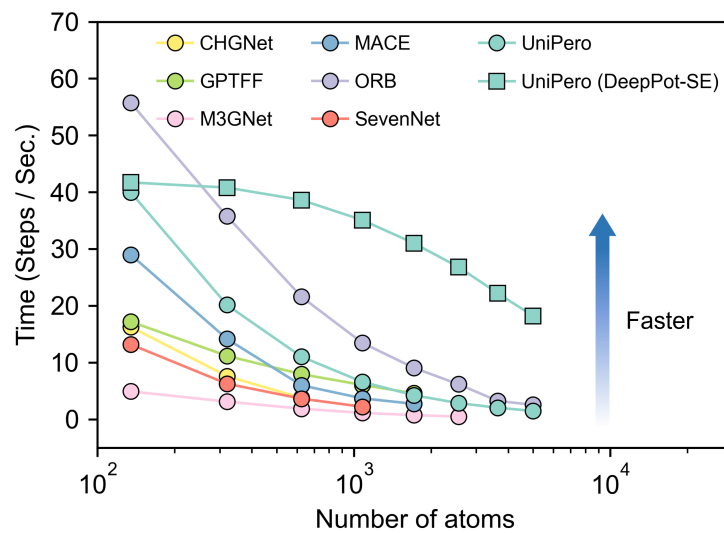


Figure 5: Computational efficiency benchmark. The reported speed data are for reference only, as a model’s optimal performance can be further improved through careful tuning and the implementation of multi-GPU parallelism.